

INTERNAL STRUCTURE OF THE MOON INFERRED FROM APOLLO SEISMIC DATA AND SELENODETTIC DATA FROM GRAIL AND LLR.

K. Matsumoto¹, R. Yamada¹, F. Kikuchi¹, S. Kamata^{2,3}, Y. Ishihara⁴, T. Iwata⁴, H. Hanada¹, and S. Sasaki⁵, ¹RISE Project Office, National Astronomical Observatory of Japan, Mizusawa, Oshu, Iwate, 023-0861 Japan (koji.matsumoto@nao.ac.jp), ²Dept. Earth and Planetary Sciences, University of California, Santa Cruz, Santa Cruz, California, 95064 USA, ³Department of Natural History Sciences, Hokkaido University, Sapporo, Hokkaido, 060-0810 Japan, ⁴Japan Aerospace Exploration Agency, Yoshinodai, Sagami-hara, Kanagawa, 252-5210, Japan, ⁵Osaka University, Toyonaka, Osaka, 565-0871 Japan.

Introduction: The knowledge of internal structure of the Moon is a key to understand the origin and the evolution of our nearest celestial body. A large amount of seismic information was brought by the near-side network consisting of four seismometers of Apollo 12, 14, 15, and 16. The Apollo seismic data have contributed to internal structure modeling, but the deepest regions which can be sounded by the travel time data are about 400 km radius (roughly 1300 km depth), leaving the structure near the center uncertain. Some studies attempted to identify the seismic wave reflected at the boundaries between fluid and solid layers by stacking noisy waveforms, e.g., [1], [2], but large differences between models still exist below the deep moonquake region.

The Moon is also observed by selenodetic techniques such as Lunar Laser Ranging (LLR), satellite gravimetry, and satellite altimetry. Lunar properties obtained from these observations include the mass, mean radius, moments of inertia (MOI), and tidal Love numbers. The recent Gravity Recovery and Interior Laboratory (GRAIL) mission has provided a degree-2 potential Love number k_2 accurate to 1% [3], [4]. This level of k_2 accuracy has a potential to better characterize the lunar deep interior [5].

The purpose of this paper is to explore lunar internal structure models which are consistent with both the seismic and the selenodetic data. The seismic travel time data will constrain crustal and mantle structures, while selenodetic data are expected to contribute to infer the structure below the deep moonquake region.

Data: We employed four selenodetically observed data of mean radius (R), mass (M), normalized mean solid moment of inertia (I_s/MR^2), and degree-2 potential tidal Love number k_2 which are reported by [6] who summarized recent results of selenodetic data analyses. The mean radius R constrains the size of the modeled Moon, and M , solid MOI, and k_2 are used, together with the seismic travel time data, to constrain the internal structure. The Love number k_2 is corrected for the anelastic contributions following [7].

We used the seismic travel time data selected by [8], i.e., 318 data (183 P-wave and 135 S-wave) from 59 sources (24 deep quakes, 8 shallow quakes, 19 meteoroid impacts, and 8 artificial impacts).

Internal structure model: Our model assumes that the Moon is spherically symmetric, elastic, and in hydrostatic equilibrium. We divide the Moon into seven shells of crust, upper mantle, middle mantle, lower mantle, low-velocity zone (LVZ), fluid outer core and solid inner core. The model parameters are the thickness, density, shear modulus and bulk modulus of each layer. We have fixed, however, some of the parameters. The boundary between upper and middle mantles and that between middle and lower mantles are fixed at 500 and 900 km depths, respectively. The density and bulk modulus of the LVZ are assumed to be the same as those of the lower mantle. The shear modulus in the fluid outer core is fixed to 0 Pa. The bulk modulus of the outer core and elastic parameters of the inner core are fixed to the model values of [1]. The density of the solid inner core is assumed to be 8000 kg/m^3 , e.g., [1], [6], but that of the fluid outer core remains variable. We prohibited models with decreasing density with depth. The number of model parameters is 18.

Inversion: A Bayesian inversion approach is an effective method to solve for a nonlinear problem such as planetary internal structure modeling, e.g., [7], [9]. This study also utilizes Markov chain Monte Carlo (MCMC) algorithm to infer the parameters of the lunar internal structure. The solutions of the parameters and their uncertainties are obtained from the posterior distribution which is sampled by the MCMC algorithm. The former is evaluated as the median value, and the latter as the 95 % upper and lower credible intervals corresponding to 2σ .

Results: Inverted results for P-wave velocity (V_p), S-wave velocity (V_s), and density are shown in Figure 1 as vertical profiles, together with probability density of each layer at certain depth. The mean crustal thickness is estimated to be $43 \pm 10 \text{ km}$. The sampled crustal density has a relatively broad distribution between 2400 and 2800 kg/m^3 . The estimated parameter values for the mantle are as follows; for the upper mantle (V_p, V_s, ρ) = $(7.62 \pm 0.09 \text{ km/s}, 4.39 \pm 0.09 \text{ km/s}, 3360 \pm 35 \text{ kg/m}^3)$, for the middle mantle ($8.03 \pm 0.12 \text{ km/s}, 4.50 \pm 0.10 \text{ km/s}, 3410 \pm 50 \text{ kg/m}^3$), and for the lower mantle ($8.27 \pm 0.22 \text{ km/s}, 4.60 \pm 0.22/-0.09 \text{ km/s}, 3490 \pm 140/-100 \text{ kg/m}^3$). The models of [1] and [2] are also shown in Figure 1 for comparison. Although slight

scatters among models are observed, averaged structures in the three mantle layers are basically consistent with each other. Our model, however, has larger lower-mantle density (Figure 1(d)).

V_S and V_P in the LVZ are estimated to be 2.6 ± 1.4 km/s and $6.9 +0.9/-0.5$ km/s, respectively. Figure 2 shows two-dimensional posterior probability function by which correlation between two parameters is depicted. A negative correlation between the outer core size and the LVZ thickness is clearly seen in Figure 2(a); a smaller outer core should be accompanied by a thick LVZ and vice versa. Consequently, an accurate independent estimate of these parameters based on current data set is challenging.

The outer core radius is estimated to be $310 +90/-200$ km and 97 % of the sampled core radius is smaller than 400 km. The thickness of the LVZ is inferred as 220 ± 170 km. The plausible inference from the existence of the LVZ is that the LVZ is partially molten where viscosity is also low and most of the tidal dissipation occurs [10, 7].

Figure 2(b) shows the correlation between the radius and density of the liquid outer core. A noticeable concentration of high probability is observed for the radius > 330 km and the density < 4500 kg/m³. This feature does not necessarily mean that this particular parameter space is the most probable, but that a larger core should have a smaller density. On the other hand, if outer core radius < 330 km the posterior probability of the outer core density tends to broadly distribute which makes it difficult to tightly constrain the density. It can be mentioned, however, that the outer core radius is likely less than 330 km if we assume that its density is larger than 5000 kg/m³ (e.g., Fe-FeS eutectic composition).

Since we assumed that the LVZ has the same density as the lower mantle, the density is estimated as an average of these two layers. The LVZ might actually have a larger density than the averaged estimate. To confirm this we conducted another inversion in which the densities (and the bulk moduli) of the lower mantle and the LVZ are estimated independently. This separated case resulted in a mantle density of $3460 +140/-50$ kg/m³ which is more consistent with previous estimates, e.g., [1], [2], and a LVZ density of 3660 ± 210 kg/m³. Although the uncertainty for the latter is large, the median value of the LVZ density at the pressure near the core mantle boundary (~ 4.5 GPa) indicates that this zone is typically high-Ti basalt which might have originated black glass with TiO₂ content ~ 16 wt% [11]. The deep Ti-rich composition is consistent with a lunar evolution model involving lunar mantle overturn in which ilmenite-bearing cumulate layer sank

with trapped incompatible heat-producing elements [12]. The above discussions support the idea that both tidal heating and radiogenic heating have maintained the partially molten region up until the present.

References: [1] Weber R. C. et al. (2011) *Science*, 331, 309-312. [2] Garcia R. F. et al. (2011) *PEPI*, 188, 96-113. [3] Konopliv A. S. et al. (2013) *JGR*, 118, 1415-1434. [4] Lemoine F. G. et al. (2013) *JGR*, 118, 1676-1698. [5] Yamada R. et al. (2014) *PEPI*, 231, 56-64. [6] Williams J. G. et al. (2014) *JGR*, 119, 1546-1578. [7] Khan A. et al. (2014) *JGR*, 119, 2197-2221. [8] Lognonne P. et al. (2003) *EPSL*, 211, 27-44. [9] Rivoldini A. et al. (2011) *Icarus*, 213, 451-472. [10] Harada Y. et al. (2014) *Nat. Geosci.*, 7, 569-572. [11] Sakamaki T. et al. (2010) *EPSL*, 299, 293-297. [12] Hess P. C. and Parmentier E. M. (1995) *EPSL*, 134, 501-514.

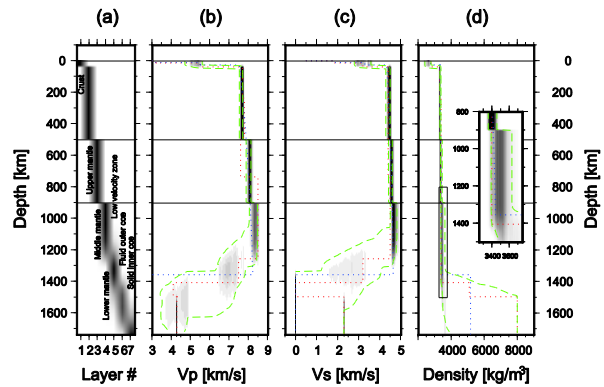


Figure 1. Vertical profiles of (a) modeled layer, (b) P-wave velocity, (c) S-wave velocity, and (d) density. Darker black color indicates higher probability of occurrence. Green broken lines indicate the 95% upper and lower credible intervals of our results. Model values of [1] and [2] are indicated as red and blue dotted lines, respectively.

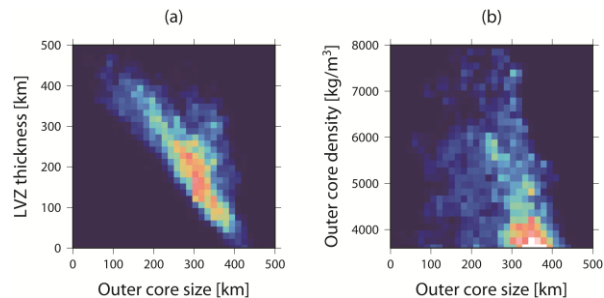


Figure 2. Two dimensional posterior probability density functions showing (a) sampled outer core radius and thickness of the low-velocity zone, and (b) sampled radius and density of the fluid outer core.